Electronic Supplementary Material (ESI) for Chemical Science.
This journal is © The Royal Society of Chemistry 2023

Nanoparticle-coated microfluidic chip for automated, non-destructive extraction of encapsulated DNA in data storage

Chunyang Geng[ab], Shaoqin Liu[*a], Xingyu Jiang[*ab]

a School of Life Science and Technology, Harbin Institute of Technology, 2 Yikuang Road, Nangang District, Harbin 150001, P. R. China.

b Guangdong Provincial Key Laboratory of Advanced Biomaterials, Department of Biomedical Engineering, Southern University of Science and Technology, No 1088, Xueyuan Rd., Xili, Nanshan District, Shenzhen 518055, Guangdong, P. R. China.

* Corresponding authors

E-mail: shaoqinliu@hit.edu.cn;

E-mail: jiang@sustech.edu.cn;

Supplementary methods

Materials. Polydimethylsiloxane (PDMS) and the curing agent were from Dow Corning (USA). The polymethyl methacrylate (PMMA) mold was fabricated by Yungu Precision Manufacturing (Shenzhen, China). SiO_2 nanoparticles with a diameter of about 30 nm were from Dibai Biotechnology (Shanghai, China). Ethyl acetate (99%), sucrose (99.9%), octadecyltrichlorosilane (OTS, 95%), 1H,1H,2H,2H-Perfluorodecyltriethoxysilane (PFDTES, 96%), and SiO_2 nanoparticles with a diameter of about 15 nm were from Macklin Biochemical (Shanghai, China). Sodium citrate (98%), calcium chloride anhydrous ($CaCl_2$, 96.0%), sodium carbonate (Na_2CO_3, 98%), iron chloride (99.9%), and ethylenediamine tetraacetic acid disodium salt dihydrate (EDTA, 99%) were from Aladdin (Shanghai, China). Absolute ethyl alcohol (99.7%) was from Sinopharm Chemical Reagent (Shanghai, China). Toluene (99.9%) was from Yonghua Chemical (Suzhou, China). Potassium ferrocyanide (99.5%) and protamine sulfate were from Yuanye Biotechnology (Shanghai, China). Ezup Column Bacteria Genomic DNA Purification Kit was from Sangon Biotechnology (Shanghai, China). HiPure PCR Pure Kit was purchased from Magen Biotechnology (Shanghai, China). *P. aeruginosa* were from Xiaohe Biotechnology (Shenzhen, China). All primers were from Generay Biotechnology (Shanghai, China). TwistAmp Basic Kit was from TwistDx (UK).

Centrifugal chip design and fabrication. We selected AutoCAD software to design the three-dimensional structure of the mold of the centrifugal chip. The production of chips adopted classical cast molding. We prepared the mixture of PDMS and the curing agent at the ratio of 10:1 (w/w) and poured it into the PMMA mold. We heated the mixture for curing at 80 °C for an hour after degassing and peeled off two layers from the PMMA mold. We treated two layers with oxygen plasma for a minute and bonded them together to construct the sealed structure.

Superhydrophobic coating fabrication. We dispersed SiO_2 nanoparticles in absolute ethanol and treated them with ultra-sonication for 30 min. After adding OTS to the solution and stirring for two hours at 60 ℃, we washed and dried the modified SiO_2 nanoparticles with absolute ethanol twice. We added modified SiO_2 nanoparticles and PDMS in ethyl acetate, treated the mixture solution with ultra-sonication and stirred for superhydrophobic coating. Fluoroalkyl silane modification has shown better hydrophobicity and even amphiphobicity. We fabricated a superhydrophobic coating with PFDTES modification and applied it in the proof-of-concept experiment of DNA data storage.

Characterization. We measured the contact angle of the coating with the drop shape analysis (KRUSS, GER) and the sliding angle with a moveable slope meter (Figure S1). We characterized morphologies of superhydrophobic coatings and calcium carbonate nanoparticles by scanning electron microscope (SEM, Hitachi S4800).

Mineralization and demineralization of DNA. We prepared a DNA solution with a concentration of 20 ng/μL by amplification and purification. The DNA solution was mixed with protamine sulfate in a ratio of 10:1 to form a stable complex. After adding calcium chloride solution in a ratio of 5:1 and mixing, sodium carbonate solution was added into the mixture and mixed by a vortex. The free DNA molecules could be encapsulated in calcium carbonate nanoparticles.

We added heparin sodium to the EDTA solution and mixed the mixture with the mineralized DNA sample. We let the mixture stand for about 15 min to release mineralized DNA.

Test of the protective effect of mineralization. We freeze-dried mineralized DNA samples on the surface of the glass and put them in the UV light box (WFH-201BJ, CHINA) and on the heating plate, respectively. After collecting samples remaining on the glass, we released DNA from mineralization samples. The decay of the DNA after treatments with UV light and high temperature could be monitored by qPCR analysis. We test the lifetime of DNA in the climate box. The environmental conditions were set as the humidity of 50% and temperature ranging from 60 to 70 ℃. We set the DNA without treatment as the control group and the concentration as C_0. We further calculated the lifetime of DNA at room temperature according to decay rates of DNA at different temperatures.

Screening primers. We designed and synthesized two primer sets for isothermal amplification of DNA fragment length of 140 nt. We amplify the amplification product after mineralization and demineralization repeatedly. After five repetitions, we compared the two primer sets by analyzing the final amplification product with gel electrophoresis and high-throughput sequencing.

Encoding and decoding data. We chose text information for concept proof of DNA data storage, and input the text file and relevant parameters such as lengths of the RS code and the data payload part, number of DNA sequences, contents of homopolymer and GC. The encoder preprocessed the binary file into a series of non-overlapping segments. Next, it iterated over Luby transform to create a single droplet containing a data payload part and a fixed-length seed, and moved to the droplet screening stage to screen the sequence for the desired biochemical properties of GC content and homopolymer runs, in which the binary droplet was translated to a DNA sequence by converting {00, 01, 10, 11} to {A, C, G, T}, respectively. It kept iterating over the droplet creation and screening steps until a sufficient number of valid oligos were generated. When decoding, we input DNA sequences encoding data and obtained the decoded file containing the original text information.

Supplementary Figures

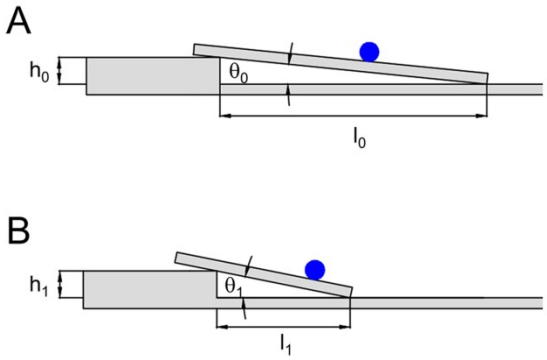

Fig. S1 Illustration of a movable slope for measuring the sliding angle. (A) Original state. θ_0, h_0, and l_0 are the angle, effective height, and slope length in the original state. (B) Position of the slope when the droplet rolled down. θ_1, h_1, and l_1 are the angle, effective height, and length of the slope at this moment.

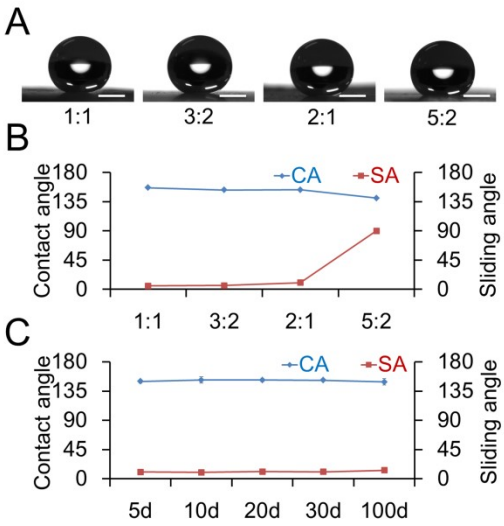

Fig. S2 Characterization of superhydrophobic coatings with different ratios and test of contact angle and sliding angle as an available time. (A) Images of droplets on the surface of PDMS modified with varying ratios of reagents. (B) Wettability of superhydrophobic coatings with different ratios of reagents (n=3). (C) Contact angle and sliding angle as an available time of superhydrophobic coatings characterized by the contact angle and sliding angle (n=3). The scale bar is 2 mm.

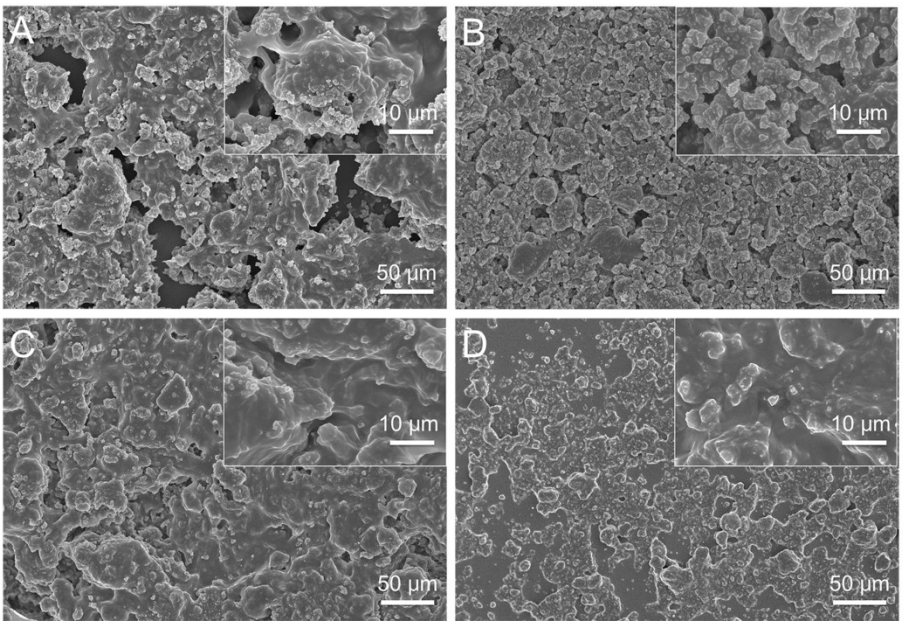

Fig. S3 SEM images of superhydrophobic coatings with different ratios. The nanostructure of superhydrophobic coatings decreased with the decreasing proportion of SiO_2 nanoparticles. The ratio of PDMS to SiO_2 nanoparticles is set as (A) 1:1; (B) 3:2; (C) 2:1; (D) 5:2.

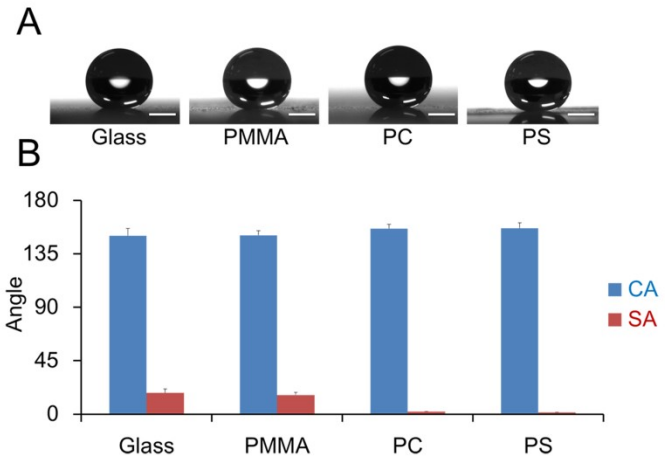

Fig. S4 Effect of superhydrophobic coatings on different materials. (A) Images of droplets on the modified surface of other materials (n=3). (B) The wettability of superhydrophobic coatings is characterized by the contact angle and sliding angle (n=3). The scale bar is 2 mm.

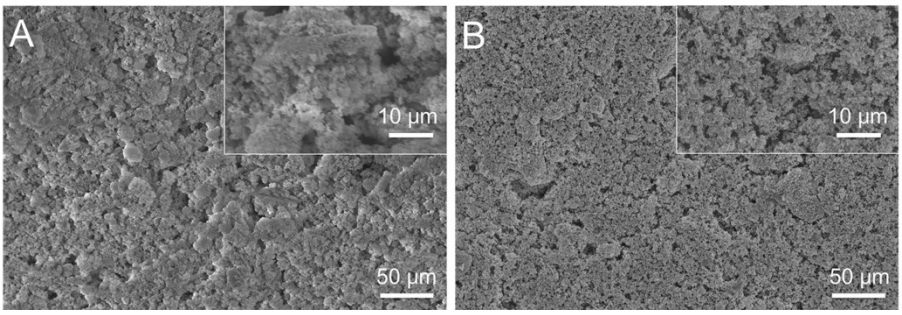

Fig. S5 SEM images of superhydrophobic coatings with ethanol as a dispersant. Ethanol generated the superhydrophobic coating with more nanostructures as a dispersant. (A) The superhydrophobic coating composed of OTS-modified SiO_2 nanoparticles. (B) The superhydrophobic coating composed of PFDTES-modified SiO_2 nanoparticles.

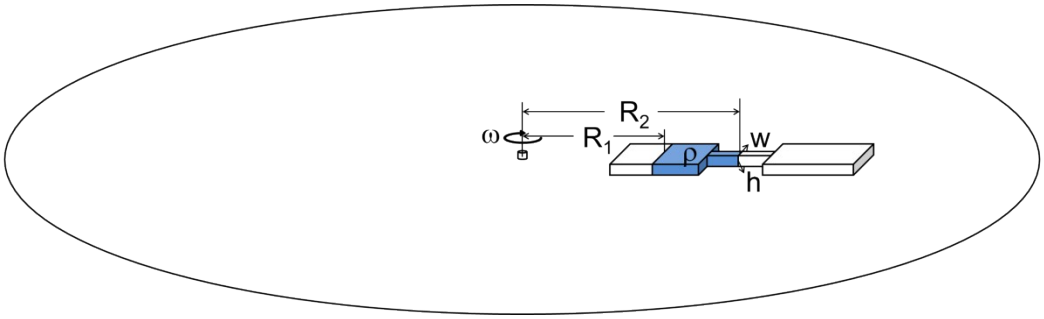

Fig. S6 Schematic diagram of liquid subjected to the centrifugal force. R_1 and R_2 are the outer and inner radii of the liquid in the channel, ρ is the density of the liquid, *w* and *h* are the width and height of the channel, ω is the rotation speed.

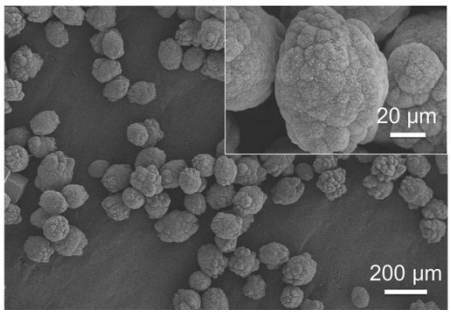

Fig. S7 SEM images of calcium carbonate nanoparticles.

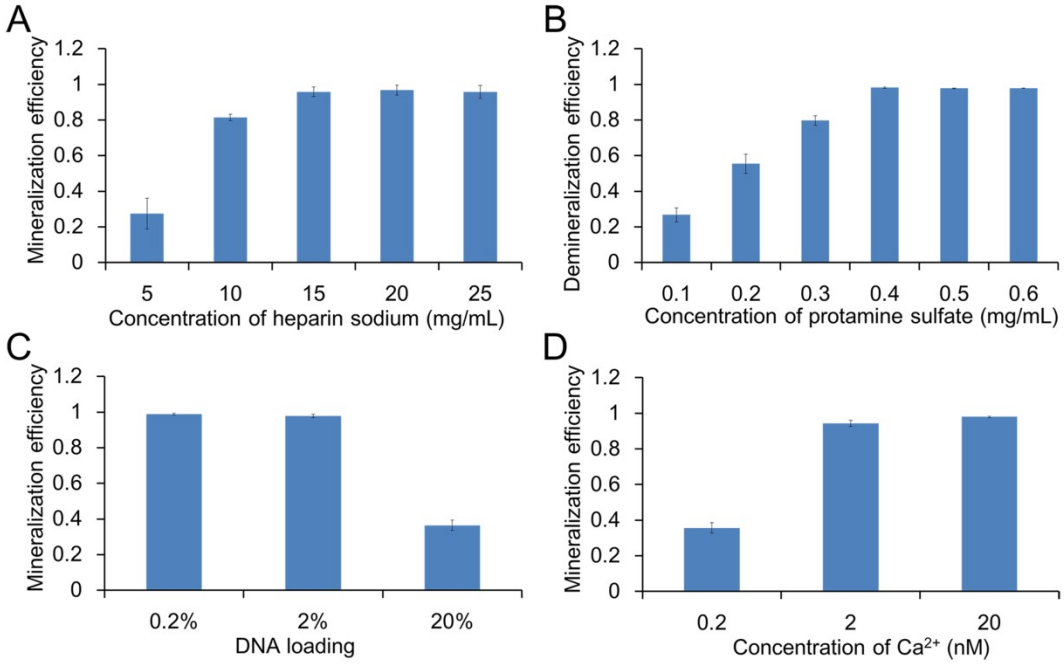

Fig. S8 Optimization of DNA mineralization and demineralization. (A) Optimization of the concentration of protamine sulfate. The combination efficiency is saturated when the concentration is over 15 mg/mL (n=3). (B) Optimization of the concentration of heparin sodium. The demineralization efficiency is saturated when the concentration is over 0.4 mg/mL (n=3). (C) Relation between DNA loading and mineralization efficiency. The mineralization efficiency of DNA decreased with decreasing concentrations of calcium chloride and sodium carbonate (n=3). (D) Optimization of the concentration of calcium chloride. The mineralization efficiency increased to nearly one hundred percent with an increasing concentration of calcium chloride (n=3).

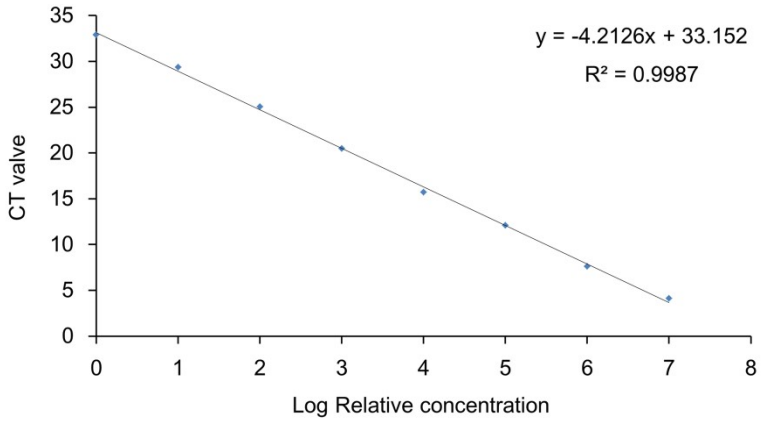

Fig. S9 qPCR CT valve as a function of DNA concentration plotted on a $\log_{10}$ axis together with data of linear fit. Reported values are averages from three technical replicates.

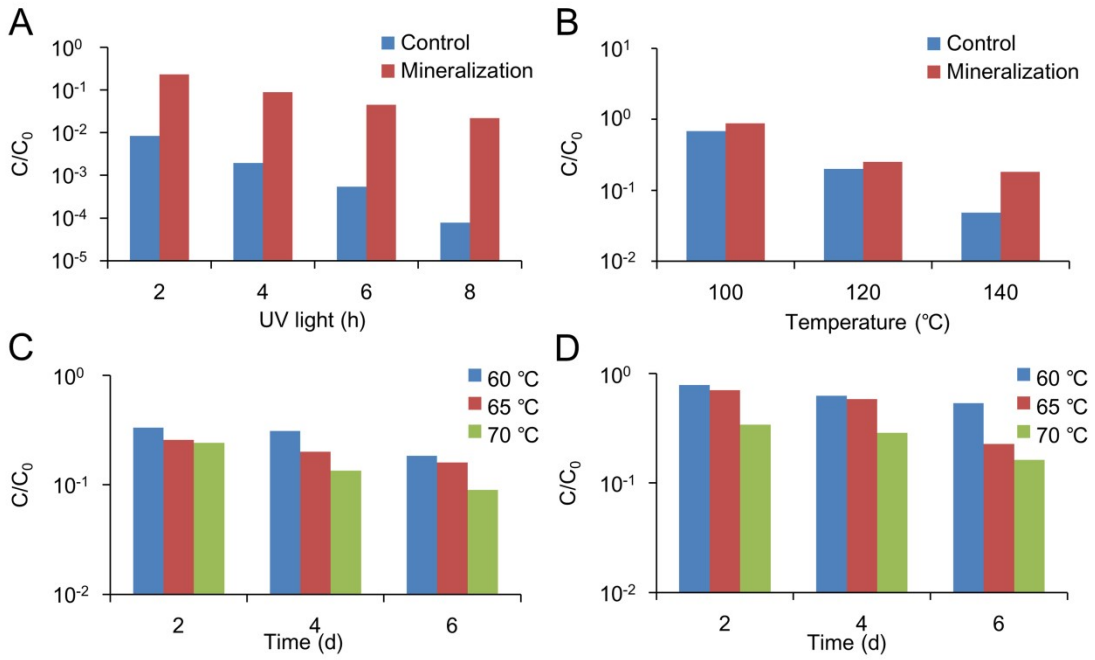

Fig. S10 Test of protective effect of mineralization. We set the concentration of DNA without any treatment as C_0. (A) Stability following UV light for up to 8 hours. The decay of DNA increased with increasing the treatment time of UV light, and the decay rate of the mineralized DNA was slower than the unprotected DNA. (B) Heat stability at temperatures from 100 to 140 ℃ for half an hour, and the decay of DNA increased with increasing the treatment time of UV light, and the decay rate of the mineralized DNA was slower than the unprotected DNA. (C) Stability of unprotected DNA in the climate box for up to 6 days. The decay of DNA increased with increasing the treatment time and environmental temperature. (D) Stability of encapsulated DNA in the climate box for 6 days. The decay of DNA increased with increasing the treatment time and environmental temperature. The decay rate of the mineralized DNA was slower than the unprotected DNA.

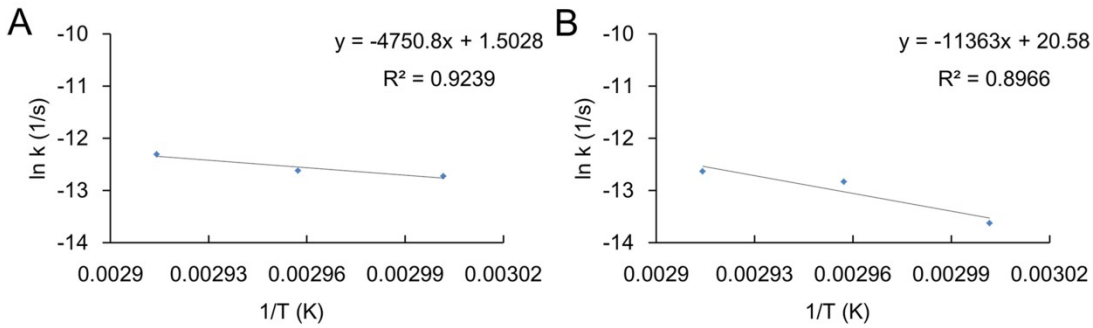

Fig. S11 Linear fit results of decay rates (ln k) to temperatures (1/T). The decay rate increased with increasing the environmental temperature. (A) The decay rate of unprotected DNA as a function of temperature ranges from 60 to 70 ℃. (B) Decay rate of mineralized DNA as a function of temperature ranging from 60 to 70 ℃.

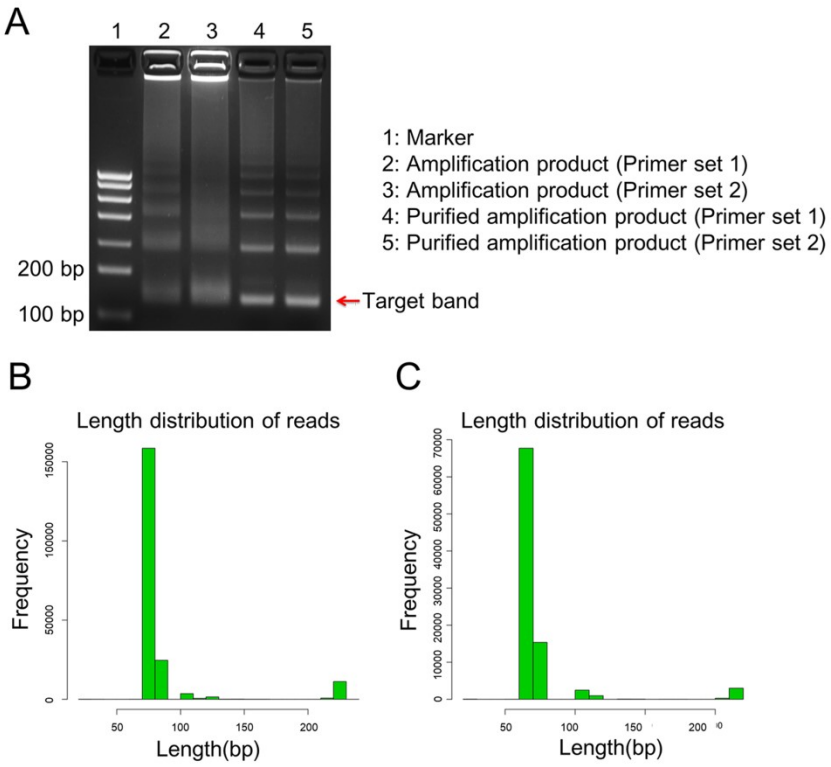

Fig. S12 Analysis of amplification products with different primers. (A) The gel electrophoresis image of amplification products. There was little difference between these two groups. (B) The high-throughput sequencing result of the amplification product with primers length of 30 nt. (C) The high-throughput sequencing result of the amplification product with primers length of 35 nt.

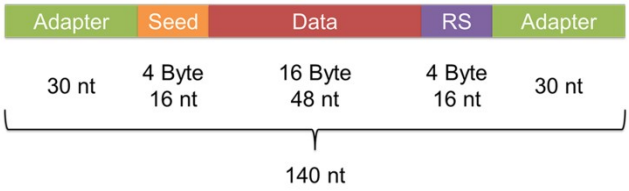

Fig. S13 Schematic diagram of the data DNA molecule.

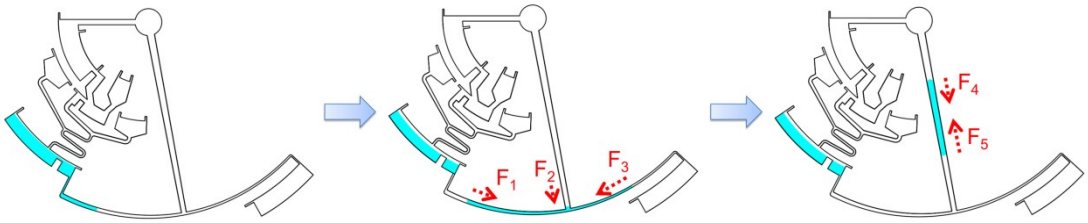

Fig. S14 Schematic diagram of transport process of the remineralized DNA sample between Fig 4E and Fig 4F. The remineralized DNA sample in the arc microchannel is subjected to capillary forces in different directions (F3>F1>F2) and driven back to the center of the circle under the resultant force (F5>F4).

Supplementary Tables

Table S1. Linear fit of concentration data to first-order decay rate expression

	k(1/s)(60 ℃)	k(1/s)(65 ℃)	k(1/s) (70 ℃)
Unprotected DNA	2.98×10^{-6}	3.32×10^{-6}	4.52×10^{-6}
DNA in calcium carbonate	1.21×10^{-6}	2.68×10^{-6}	3.26×10^{-6}

Table S2 Linear fit of decay rate data to yield Arrhenius activation energies and the pre-exponential factors (ln(k) vs. 1/T).

	Ea(kJ/mol)	k_0(1/s)
Unprotected DNA	39.50	4.49
DNA in calcium carbonate	94.47	8.67×10^{8}